LUMINESCENCE AND RAMAN STUDIES OF ZnSe/ZnS MULTIPLE QUANTUM WELL STRUCTURES

Th. Weber, H. Stolz and W. von der Osten
Fachbereich Physik, Universität-GH, W-4790 Paderborn, Germany

Zhao Futan and Shen Yongrong
Laboratory of Excited State Processes, Changchung Institute of Physics CAS, P.R. China

(Received 7 December 1992)

We present luminescence and Raman spectra of ZnSe/ZnS quantum wells fabricated by metal organic chemical vapour deposition. Our experiments provide information on the structure of the sample interfaces between adjacent layers. Especially LO phonon Raman scattering is found to be sensitive to strain and to the undesired formation of a solid solution between the two compounds. A calculation using a one-dimensional particle-in-box model with finite barriers gives good agreement with the measured exciton energies assuming as fitting parameter a valence band discontinuity of 91%.

1 Introduction

In the last decade, semiconductor quantum well structures have entered into micro- and optoelectronic device technology. Directed towards optoelectronic applications in the near-infrared spectral region, so far layered structures or quantum wells mainly of III/V-semiconductors and of silicon became of practical use and can be fabricated in high quality by refined production techniques. It is only recently that efforts are undertaken to also develop II/VI-semiconductor structures which have wider bandgaps and would extend the spectral range into the visible. In particular, the latest success in p-doping of ZnSe layers [1, 2] and the fabrication of visible light emitting diodes and laser structures [3] has initiated increased interest in these materials and shown the necessity to test structures produced by different techniques.

Material	Bandgap/eV	m_e^*	m_{hh}^*
ZnSe	2.82	0.17	0.6
ZnS	3.82	0.34	0.49

Table 1: *Bulk material parameters of ZnSe and ZnS for T=2K.*

In this paper we present investigations of the luminescence and Raman spectra of ZnSe/ZnS quantum wells that were fabricated by metal organic chemical vapour deposition. In this system, ZnSe forms the quantum well while ZnS is the barrier material (cf. Table 1). While the large bandgap of the two materials, as opposed to other II/VI combinations, guarantees light emission up to the near ultraviolet, a major problem is the relatively large lattice mismatch. ZnS has a nearly 5% smaller lattice constant than ZnSe which results in considerably strained layers near the interface to the substrate. Starting from a critical layer thickness, dislocations develop that relax the strain [4]. These dislocations, however, represent an additional perturbation in the sample which will result in non-radiative relaxation processes that reduce the quantum efficiency of any optoelectronic device. We therefore have studied quantum wells having relatively small wellwidths so that higher sample quality can be expected.

2 Experimental

In our spectroscopic examinations, excitation was accomplished by a tunable dye laser which was pulsed providing pulse durations of 6 ps. It was synchronously pumped by a mode-locked frequency tripled Nd^{3+}:YLF laser system and, with Stilbene 3 or Exalite 392E as active media, worked in the wavelength ranges 420nm–460nm (2.95–2.69eV) and 378nm – 395nm (3.12 – 3.28eV), respectively. In addition, direct exci-

0749-6036/93/030359+05 $08.00/0

tation with the frequency tripled pump laser at 351nm (3.5eV) was used. The spectral analysis of the emitted light was performed by a 1m double monochromator. In the time–resolved measurements the time resolution was limited by the response of our set–up which amounts to about 20 ps with a microchannel-plate multiplier as photodetector [6]. The samples were mounted in a He–flow cryostat which allowed a temperature variation from 1.6K to 300K. We investigated samples grown by metal organic chemical vapour deposition with GaAs or CaF_2 as substrate materials. As the samples with GaAs substrate had better quality, we here report the results obtained for these, especially for a sample with 30 periods of ZnSe/ZnS. The well and barrier widths are nominally 2 nm and 25 nm, the optical measurements indicating slight deviations from that.

3 Results and discussion

3.1 Photoluminescence and Raman scattering spectra

The low temperature photoluminescence spectrum of the 2 nm/25 nm ZnSe/ZnS sample excited at an energy E_L = 3.5eV essentially shows four emission bands (Fig. 1), all situated well above the bulk ZnSe-bandgap (cf. Table 1).

Based on the resonant enhancement of phonon scattering described below, the most prominent band A is ascribed to the lowest exciton state in the ZnSe quantum well with the low energy shoulder due to bound states. The much less intense band B has similar line-

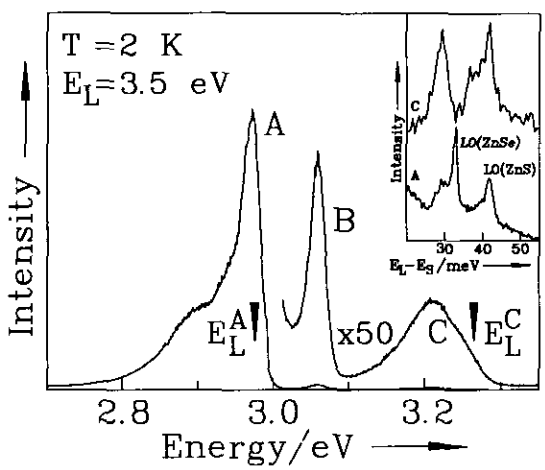

FIGURE 1: *Luminescence spectrum of a ZnSe (2nm)/ ZnS (25nm) multiple quantum well structure at T=2K. The high energy part is multiplied by a factor 50. The arrows mark the excitation photon energies for the Raman spectra displayed in the inset.*

shape like A from which we conclude that it is also of excitonic nature, but very probably originates from wells with different (smaller) wellwidth (see below). Line C differs distinctly from A and B. It is broader by a factor of 3 and also very weak. We find the lifetimes of all emission lines not significantly different from each other and about 300 ps.

E_L^A and E_L^C mark the laser excitation photon energies to produce the Raman spectra A and C, respectively, displayed as the inset of Fig. 1. The two lines in each spectrum are due to LO–phonon scattering with the phonons propagating in ZnSe and ZnS as indicated. For resonant excitation in the region of the emission band A, the measured LO(ZnSe) energy (33.0 meV) is larger than the bulk value (31.8 meV), while the measured LO (ZnS) phonon (42.0 meV) has smaller energy than in bulk ZnS (44 meV) [7]. This contrasts to excitation in band C, where the LO (ZnSe) phonon is shifted to lower energy (30 meV) like the LO(ZnS) phonon, which is a well–known behaviour in $ZnSe_xS_{1-x}$ solid solutions [7].

An important observation concerning the interrelation between the emission bands A and C is that no intensity enhancement at all is found for line A under excitation in band C (at E_L^C). From this and the Raman data we conclude that A and C are not related but rather result from states in different layers. The excitonic state A is localized in a quantum well characterized by smooth interfaces between ZnSe and ZnS, while C is caused by states in wells with solid solution character and, hence, lower quality.

To further check if line A originates from exciton states in the ZnSe quantum well, we employed Raman spectroscopy under resonant excitation in the range of band A. Due to exciton–phonon coupling, in this case one would expect a strong enhancement of the LO(ZnSe) Raman process, while LO(ZnS) phonon scattering should not be enhanced. The spectra in Fig. 2 obtained for different excitation photon energies, together with the Raman profile in Fig. 3, completely confirm this expected behaviour. More specifically one observes a strong enhancement of the LO (ZnSe) Raman line if the scattered photon energy is equal to the exciton energy ("outgoing resonance"). Besides, there occurs an appreciable broadening of this line which in resonance becomes about 3 meV (FWHM) wide. This broadening agrees fairly well with the range of energies of the LO(ZnSe) phonons confined in a quantum well about 2 nm wide. The incoming resonance of the LO(ZnSe) phonon process is weaker as usual. No resonance at all is found for the LO(ZnS) phonon scattering. All these observations support our interpretation. In particular, the measured shift of the LO(ZnSe) and LO(ZnS) phonon to higher and lower energies, respectively, is explained by the lattice mismatch between adjacent ZnSe and ZnS

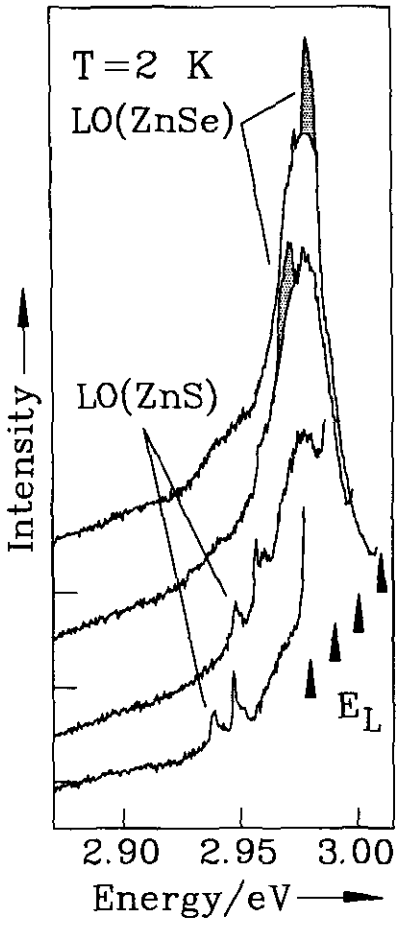

FIGURE 2: *Luminescence and Raman spectra under resonant excitation in band A at the laser photon energies E_L marked by arrows.*

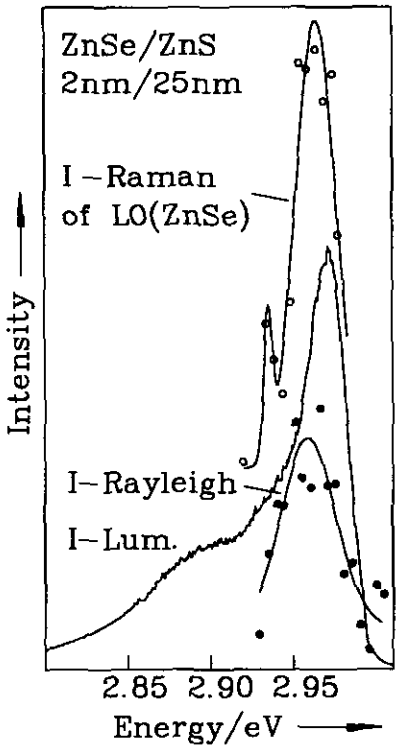

FIGURE 3: *Resonance Raman (circles) and Rayleigh (full points) profiles in comparison with the luminescence lineshape of emission band A. The full lines are guidelines for the eye. Zero suppressed for Raman and Rayleigh profile. T=2K*

layers. The mismatch leads to lateral strains near the interfaces resulting in both a compression of the ZnSe lattice and tension of the ZnS lattice consistent with the changes in LO phonon energies.

In contrast, under resonant excitation in band C (Fig. 1), the Raman signal of both ZnSe and ZnS phonon branches is enhanced. It confirms that this band results from excitons localized in less strained quantum wells with unintentionally present solid solution character.

Besides providing information on the Raman processes, the selective excitation measurements in Fig. 2 demonstrate that the exciton band A is inhomogeneously broadened ($\delta E_{inh} \simeq 30\ meV$). Lowering the excitation photon energy E_L results in a fluorescence line narrowing typical for inhomogeneously broadened optical transitions because it implies that emission in each spectrum stems from states lower in energy than E_L. The inhomogeneous nature of the excitons is confirmed by our measurements of resonant Rayleigh scattering. As has been shown for III-V quantum well structures [6, 8, 9], this process is due to spatial static disorder in the interface and becomes strongly enhanced for excitonic resonances. Fig. 3 shows the Rayleigh profile measured for the ZnSe/ZnS quantum well. It exhibits a clear resonance across the exciton band with the width of the profile being roughly equal to δE_{inh}.

3.2 Temperature dependence of spectra

Temperature dependent luminescence spectra give information on the possible activation processes and corresponding activation energies. Assuming a Boltzmann type behaviour, the luminescence intensity originating from state j at energy E_j as function of temperature may be written as

$$I_j(T) \sim \frac{1}{1 + \sum_{i \neq j} (g_i \Gamma^{\infty}_{ji} / g_j \Gamma^{tot}_j) exp(-\Delta E_{ij}/kT)}. \quad (1)$$

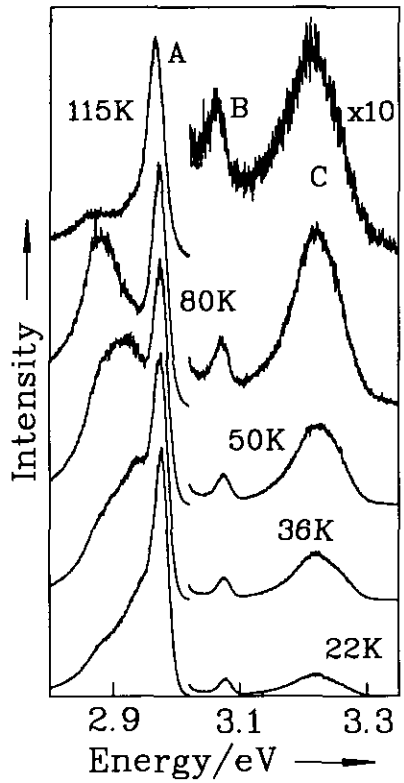

FIGURE 4: *Luminescence spectra at different temperatures normalized in (peak) intensity to exciton line A. The high energy part of the spectra are all multiplied by a factor of 10.*

Here $\Delta E_{ij} = E_i - E_j$ denotes the activation energy into state i, g_i and g_j are degeneracy factors, Γ_{ji}^{∞} is the probability for a transition j→i at T→ ∞ and Γ_j^{tot} the total transition probability of state j. The sum runs over all energy states of the system, however, since for most states $\Delta E_{ij} \gg$kT or the ratio $g_i\Gamma_{ij}^{\infty}/g_j\Gamma_j^{tot}$ is small, in practice only a few activation processes will be relevant.

Fig. 4 displays spectra at different temperatures normalized to the intensity of line A. Concerning the low energy shoulder associated with this line, these spectra reveal that it consists of several components which we ascribe to bound states. Their temperature behaviour is characterized by thermal redistribution among the states which finally, at 115K, are nearly depopulated. Up to about 100K besides a 10 meV shift of all lines to lower energies, the main temperature effect is an intensity reduction as shown over the whole temperature range in Fig. 5. Applying eq.(1) to fit these data, not quite satisfactory agreement is obtained by taking into account only one activation energy (ΔE_{act}^1 in Table 2). The fits are improved in the low temperature region

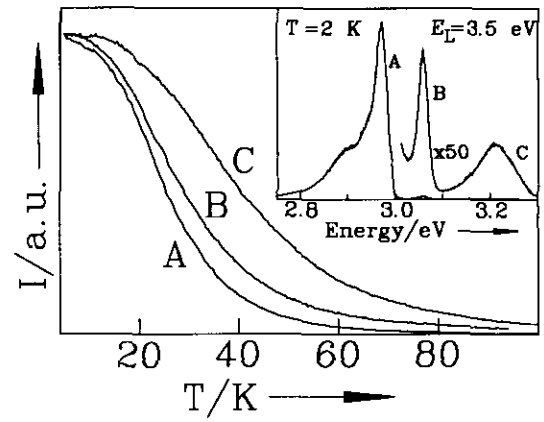

FIGURE 5: *Luminescence peak intensities of emission bands A, B and C as function of sample temperature. All intensities are normalized to their low temperature values.*

using two activation processes with activation energies ΔE_{act}^1 and ΔE_{act}^2 (Table 2) and corresponding relative weighting factors of about 90:1. States A and C have an activation energy of 40 meV in common, in contrast to the 20 meV activation energy for line B. The second activation energy for each line is much smaller (10 meV for A and C, 2meV for B),but contributes only little.

3.3 Model calculation of energy states

To calculate the energies of the confined exciton states, we treated the ZnSe/ZnS quantum well system as a particle in a one-dimensional box with finite barriers and continuous boundary conditions for the particle wavefunction and velocity. The energies not only depend on

Line	A	B	C
measured E/eV	2.97	3.06	3.22
calculated E/eV	2.99	3.07	
$\Delta E^1{}_{act}$/meV	40	20	40
$\Delta E^2{}_{act}$/meV	10	2	10

Table 2: *Comparison of calculated and experimental values of various quantities for excitonic states A, B and C. E: energy positions of states. ΔE_{act} : activation energies. For each transition the relative strength of the activation processes 1 and 2 is about 90:1.*

the effective carrier masses and bandgap energies (Table 1). Also exact values of the wellwidth, of the exciton binding energy and for the ratio of the potential discontinuities in the valence and conduction bands must be known.Ascribing the 40meV and 20meV measured

for state A and B to the exciton binding energy in the confined system (as opposed to ≈ 20meV in ZnSe bulk material [7]), we calculated the energy positions of the exciton states for wellwidths of 6 and 5 monolayers corresponding to 17 nm and 14.2 nm, respectively, close to the nominal width. Under the reasonable assumption of a valence band discontinuity between adjacent ZnSe and ZnS layers of 91% [5], which enters as the only free fitting parameter into the calculation, we got very good agreement with the measured energies of lines A and B supporting our assignment above (cf. Table 2).

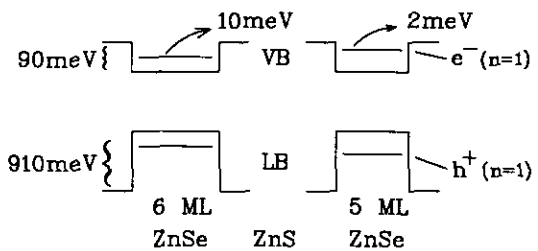

FIGURE 6: *Discontinuities of conduction and valence band (CB, VB) assumed to calculate the energies of states in ZnSe/ZnS quantum wells with 6 and 5 ZnSe monolayers (ML).*

Due to the small electron effective mass and conduction band discontinuity, the electron is only weakly localized in the ZnSe well (Fig. 6). We find from our calculation that the localization energies of the lowest electron state are 10 and 2 meV for the two layer thicknesses in excellent agreement with the measured activation energies. This suggests that, subsequent to relaxation into confined electron-hole states, exciton formation takes place concurrent with thermal activation of the electron to continuum states extending into the barrier. In addition the smaller exciton binding energy found for state B in comparison to A would qualitatively be consistent with our assignment, as the less-confined electron corresponds to a more extended wavefunction and, hence, a smaller value of the exciton binding energy.

As implied by eq.(1), the intensity reduction does not only depend on the activation energy, but also on the prefactor $g_i\Gamma_{ji}^{\infty}/g_j\Gamma_j^{tot}$. This factor is determined by the cross-section for the capture of a completely free exciton at the binding center i and certainly will be important for any practical application of the ZnSe/ZnS quantum well system.

4 Concluding Remarks

As to the realization of efficient light sources based on ZnSe/ZnS heterostructures, one is concerned with two major problems. One is that obviously nonradiative recombination processes still affect the lifetime which for all investigated transitions in our sample was small even at very low temperatures and most possibly is related to the strain in the sample. Also the activation energies, in particular the electron confinement energies, are small causing a drastic reduction of the quantum efficiency of the excitonic states at higher temperatures. Both these features presently would not allow one to produce an efficient light source.

References

[1] R.M. Park, M.B. Trofer, C.M. Rouleau, J.M. DePuydt and M.A. Haase, Appl. Phys. Lett. 57 (1990) p. 2127.

[2] M. Haase, J. Qui, J.M. DePuydt and H. Cheng,Appl. Phys. Lett. 59 (1991) p. 1272.

[3] H. Jeon, J. Ding, W. Patterson, A. Nurmikko, W. Xie, D. Grillo, M. Kobayashi and R.L. Gunshor, Appl. Phys. Lett. 59 (1991) p. 3619.

[4] Yoichi Kawakami, Tsunemasa Taguchi and Akio Hiraki, J.Cryst.Growth, 93 (1988) p. 714.

[5] K. Shahzad, D.J. Olego and C.G. Van de Walle, Phys. Rev B, Vol.38, No.2 (1988) p. 1417.

[6] H. Stolz in: Advances in Solid State Physics, Vol. 31 ed. by U. Rössler (1991) p. 219.

[7] II-VI Compounds, Landolt-Börnstein, Numerical Data and Functional Relationships in Science and Technology New Series III 17b Semiconductors ed. by O. Madelung (1982) p. 171.

[8] H. Stolz, D.Schwarze, W. von der Osten and G.Weimann, Supperlattices and Microstructures, Vol.9, No.4 (1991) p.511

[9] J. Hegarty, M.D. Sturge, C. Weisbuch, A. Gossard and W. Wiegmann, Phys. Rev. Lett 49,930 (1982)